



# Studies on phase change $\text{Se}_{80}\text{In}_5\text{Te}_6\text{Sb}_9$ thin films by $\gamma$ -irradiation for optoelectronic devices

Archana Srivastava\*

Department of Physics, St. Andrews College, Gorakhpur, U.P. 273001, India

## Abstract

In this research work, we have synthesized bulk  $\text{Se}_{80}\text{In}_5\text{Te}_6\text{Sb}_9$  alloy using melt quenching technique and these films having thickness 400 nm were coated on glass substrate using thermal evaporation technique. The amorphous as well as glassy nature of synthesized  $\text{Se}_{80}\text{In}_5\text{Te}_6\text{Sb}_9$  alloy was confirmed by non-isothermal DSC measurements at different heating rates 5, 10, 15, 20 K/min. The phase transformation studies in  $\text{Se}_{80}\text{In}_5\text{Te}_6\text{Sb}_9$  thin films were studied by inducing  $\gamma$ -irradiation of doses 4, 8, and 12 kGy at dose rate of 2 kGy/hr using Gamma chamber (GC-5000). The structural, morphological and optical studies of as-prepared and  $\gamma$ -irradiated thin films were studied by High resolution X-ray diffraction (HRXRD), Field Emission Scanning Electron Microscopy (FESEM) and UV/VIS/NIR spectrophotometer respectively. The optical parameters such as absorption coefficient and extinction coefficient were found to be vary with  $\gamma$ -irradiation doses. The optical band gap is found to be increased as  $\gamma$ -irradiation doses increases. These notable shifts in the optical band gap and absorption coefficient values can be explained by the increase in disorderness and lattice strain due to  $\gamma$ -irradiation.

**Key words:** Chalcogenide glass, Thin films, Absorption coefficient, Band gap, Phase Transformation

\*Corresponding author e-mail: [dr.archanaphys@gmail.com](mailto:dr.archanaphys@gmail.com)

## 1. Introduction:

During the past decades, a lot of research works have been done on the chalcogenide alloys due to their structural flexibility and phase reversibility [1-2] properties. These glasses have a significant influence on science and technology due to their extensive applications, including in solar cells, infrared detectors, optical recording media, and image processing systems [3-6]. Significant research has focused on the development of novel chalcogenide materials with tunable physical and chemical properties, which form the basis for next-generation solid-state devices [7]. The primary application of these glasses is in the field of optics due to their infrared transmission capabilities and photo-induced phenomena [8-9]. Chalcogenide glass (ChG) thin films have attracted researcher's significant interest due to their versatile functionalities in advanced electronic and photonic innovative technologies [10-11]. The absorption coefficient, optical band gap and extinction coefficient are the most noteworthy parameters in chalcogenide thin films for investigating their applicability. Chalcogenide thin films undergo notable changes in their optical constants upon exposure to gamma radiation, making them highly suitable for a range of technological and research applications.

These changes are particularly crucial for holographic optical data storage and the fabrication of various integrated devices and components [12-14]. Extensive research has been conducted on chalcogenide thin films in which Selenium is the predominant element [15-18]. Hagari et al. [19] have studied the effect of the  $\gamma$ -irradiation exposure by 100–500 kGy doses on the optical properties and single oscillator parameters for Se-S-Sb thin films. The absorption coefficient was found to increase with the increase of the doses of  $\gamma$ -radiation. Ahmad et al. [20] have studied the influence of different doses of gamma irradiation on optical and structural properties of thermally evaporated CdSe chalcogenide thin films. They have found the increase in optical band gap and variation in other optical parameters like refractive index ( $n$ ), extinction co-efficient ( $k$ ), absorption co-efficient ( $\alpha$ ) and Urbach energy ( $E_u$ ) with gamma irradiation. Shpotyuk et al. [21] done the optical studies of As-S chalcogenide glasses under the effect of gamma irradiation. Non-crystalline In-Cd-Se thin films were irradiated by 60 Co  $\gamma$ -rays at different doses (100–400 kGy) by Aly et al. [22]. The absorption coefficient was discovered to rise as the gamma doses were increased. The decrease in the optical energy gap with the  $\gamma$ -doses was attributed to the rise in the defects after irradiation. The alteration in optical properties of Ag-Sb-Se thin films irradiated by  $\gamma$ -radiation was studied by Abdul-Kader et al. [23]. It was established that exposure of  $\gamma$ -radiation leads to increase in refractive index. Optical absorption analysis exposed the presence of an indirect transition with decreasing band gap on increasing  $\gamma$ -dose. The irradiation effect of  $\gamma$ -rays on Se-Sn glass with different doses has been explored by Al-Ewaisi et al. [24] and they found an allowed indirect optical band gap, which increased up to 20 kGy after which  $E_g$  decreases. The chalcogenide thin films from Se-Te-In glasses have received considerable attention owing to their exceptional scientific and technological applications, including optical data storage, phase-change memories and photonic devices [25-27]. Introducing Antimony (Sb) into the Se-In-Te ternary chalcogenide glass system transforms it into a quaternary alloy which offers improved optical transparency, tailored phase-change behaviour and enhanced thermal stability.

This study investigates the phase change studies of  $\text{Se}_{80}\text{In}_5\text{Te}_6\text{Sb}_9$  quaternary chalcogenide thin films by inducing  $\gamma$ -irradiation, with selenium (Se) as the primary element due to its technological relevance, strategic importance in optoelectronics, and its natural tendency to form stable glassy materials. Selenium based materials offer significant advantages for commercial and technological applications due to their high glass-forming ability, enhanced thermal stability [28] and wide transparency window [29]. However, pure Se suffers several drawbacks. To overcome these limitations, we have added indium (In) and tellurium (Te) to form Se-In-Te ternary compound as a base due to its versatility and wide range of applications. This study further explores the incorporation of antimony (Sb) into the Se-In-Te system, leveraging Sb's known use in low-melting alloys for applications such as automatic fire sprinkler systems, electrical fuses and fire detection systems.

## 2. Experimental:

We have synthesized  $\text{Se}_{80}\text{In}_5\text{Te}_6\text{Sb}_9$  chalcogenide glass from highly pure (99.999%) Se, In, Te and Sb elements using melt quenching technique. The appropriate amount of elements was weighed conferring to their atomic percentage and kept into ultrasonically cleaned quartz ampoules. Further, we have sealed the ampoules under a vacuum of  $10^{-5}$  Torr and placed them in a microprocessor-controlled electric furnace, which operated in four steps. In the first step, the temperature was maintained at 673 K for 2 hours; in the second step, it was raised to 873 K for 2 hours; in the third step, it was set to 973 K for 3 hours; and finally, in the fourth step, the temperature was increased to 1023 K for 3 hours. The ampoules were periodically agitated during melting to promote homogeneity of the melt. The ampoules

containing the molten materials were rapidly quenched in ice-cooled water to capture the melt structure. Then we have grinded the ingots into fine powdered form by using pastel and mortar. Differential Scanning Calorimeter (Model–DSC plus, Rheometric Scientific Company, U.K) has been used for confirming the glassy as well as amorphous nature of  $\text{Se}_{80}\text{In}_5\text{Te}_6\text{Sb}_9$  alloy at different heating rates of 5, 10, 15 and 20 K/min. Thin films (thickness = 400 nm) of glassy alloy of  $\text{Se}_{80}\text{In}_5\text{Te}_6\text{Sb}_9$  were prepared on ultrasonically cleaned glass substrate by using thermal evaporation technique, whose thickness was measured by a quartz crystal thickness monitors (Edward model FTM 7). Thin films of  $\text{Se}_{80}\text{In}_5\text{Te}_6\text{Sb}_9$  glasses were irradiated by gamma ( $\gamma$ ) rays with 4, 8, and 12 kGy doses at a dose rate of 2 kGy/hr using Gamma chamber (GC-5000) for phase transition studies. The Regaku X-ray diffractometer Ultima IV was used for structural analysis of as-deposited and  $\gamma$ -irradiated thin films. X-ray diffraction (XRD) measurements were performed using a copper target ( $\text{Cu K}\alpha_1$ ,  $\lambda = 1.54178 \text{ \AA}$ ) as the radiation source. The scan range was set from  $20^\circ$  to  $60^\circ$  ( $2\theta$ ) with a scanning speed of  $2^\circ/\text{min}$  and a chart speed of 1 cm/min. The surface morphology of the thin films during the phase transformation was characterized by Field Emission Scanning Electron Microscope (FESEM, QUANTA FEG 450, Amsterdam, Netherlands). A JASCO spectrophotometer was employed for optical absorption studies of as-prepared and  $\gamma$ -irradiated thin films in 400-1100 nm wave length.

### 3. Results and discussion

#### 3.1: Structural and morphological properties:

Fig. 1 presents the DSC curves of  $\text{Se}_{80}\text{In}_5\text{Te}_6\text{Sb}_9$  glasses recorded at these different heating rates of 5, 10, 15 and 20 K.min. The existence of sharp glass transition and crystallization peaks approves the amorphous as well as glassy nature of the prepared alloy.

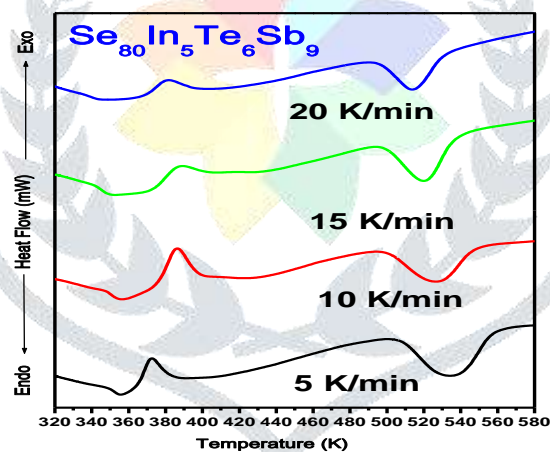


Fig. 1: DSC plot of  $\text{Se}_{80}\text{In}_5\text{Te}_6\text{Sb}_9$  alloy at different heating rates.

The HRXRD diffraction patterns of as-deposited and  $\gamma$ -irradiated  $\text{Se}_{80}\text{In}_5\text{Te}_6\text{Sb}_9$  thin films are shown in Fig. 2. The absence of sharp structural peak in HRXRD pattern in as-deposited film is approving its amorphous structure.

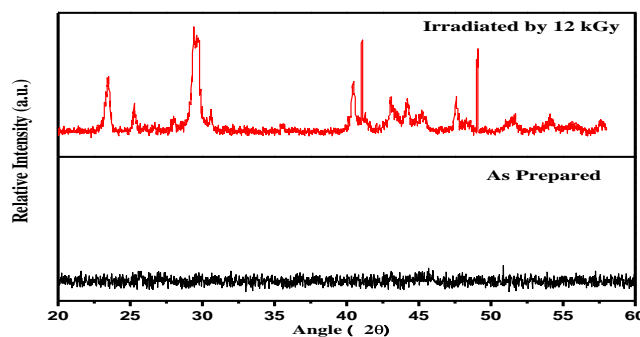


Fig 2: HRXRD Patterns of as-prepared and Gamma irradiated  $\text{Se}_{80}\text{In}_5\text{Te}_6\text{Sb}_9$  thin films.

On the other hand, the  $\gamma$ -irradiated films have sharp structural peaks confirming the crystallization phases due to gamma exposure. The intensity of the diffraction peaks increased at higher doses.

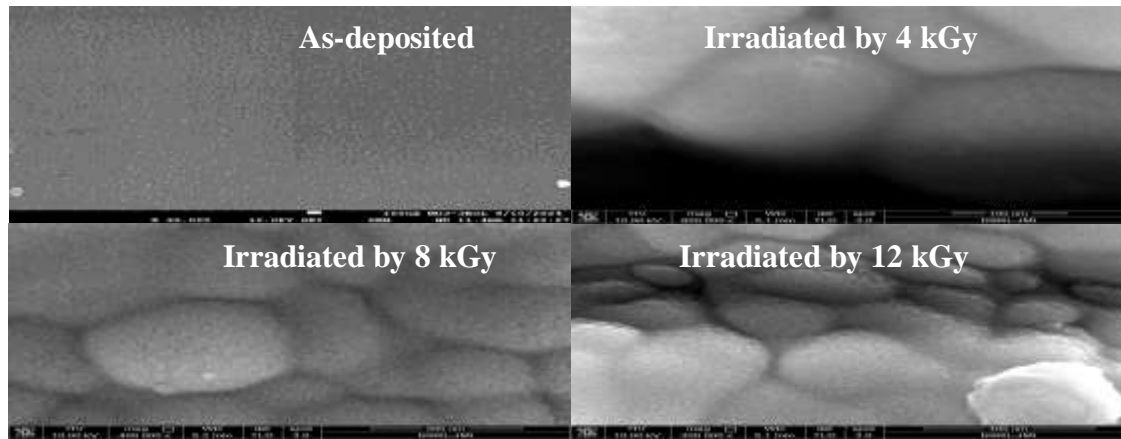


Fig. 3: FESEM images of as-deposited and  $\gamma$ -irradiated  $\text{Se}_{80}\text{In}_5\text{Te}_6\text{Sb}_9$  thin films at different doses.

Field Emission Scanning Electron Microscopy (FESEM) is a powerful technique for morphological analysis, offering critical insights into the growth mechanisms, size and shape of samples. Its combination of high magnification, substantial depth of field and exceptional resolution makes FESEM an indispensable tool in materials characterization.

To investigate the alterations in surface morphology associated with  $\gamma$ -irradiation phase transitions in  $\text{Se}_{80}\text{In}_5\text{Te}_6\text{Sb}_9$  glassy alloys, we employed FESEM. Fig. 3 presents the FESEM micrographs of as-deposited and  $\gamma$ -irradiated  $\text{Se}_{80}\text{In}_5\text{Te}_6\text{Sb}_9$  thin films. Morphological analysis of the as-deposited  $\text{Se}_{80}\text{In}_5\text{Te}_6\text{Sb}_9$  thin films revealed a smooth, crack-free surface devoid of agglomerates or precipitates, indicating the absence of secondary phases. This observation was corroborated by FESEM micrographs, which confirmed the uniformity and purity of the as-grown films. In contrast, FESEM images of  $\gamma$ -irradiated thin films distinctly displayed the emergence of crystallites with well-defined facets. This morphological transformation is likely attributed to  $\gamma$ -irradiation induced nucleation and subsequent grain growth, a phenomenon consistent with previous studies where gamma irradiation has been shown to enhance crystallinity and promote grain coalescence in various thin film materials [30].

### 3.2: Optical studies:

The optical characterization plays a pivotal role in evaluating various optical parameters of  $\text{Se}_{80}\text{In}_5\text{Te}_6\text{Sb}_9$  thin films. Spectrophotometry instrumentation is the key technique for the determination of absorption coefficient and extinction coefficient, which are essential for understanding the material's optical behavior and optimizing its performance in applications. Absorbance measurements serve as a fundamental tool for determining optical parameters, including the absorption coefficient, optical band gap and extinction coefficient. By analyzing the absorbance spectra, one can estimate the amount of light absorbed by thin films under specific conditions. At the absorption edge, electrons are excited from lower to higher energy levels upon interaction with photons of known energy, facilitating the assessment of electronic transitions within the material.

We have used a JASCO spectrophotometer of photometric accuracy 0.004 for determining the optical absorption spectra of as-prepared and  $\gamma$ -irradiated  $\text{Se}_{80}\text{In}_5\text{Te}_6\text{Sb}_9$  thin films within the wavelength span 400 nm–1100 nm. Absorbance quantifies the amount of light absorbed by a sample under specific conditions, providing critical insights into the sample's optical properties.

The absorption coefficient ( $\alpha$ ) was calculated by following equation [31]:

$$\alpha = \text{Optical density} / \text{thickness of the film} \tag{1}$$

We have plotted a graph of absorption coefficient ( $\alpha$ ) versus photon energy ( $h\nu$ ) for as-prepared and  $\gamma$ -irradiated  $\text{Se}_{80}\text{In}_5\text{Te}_6\text{Sb}_9$  thin films (shown in Fig. 4). It is clear from this figure that absorption coefficient ( $\alpha$ ) increases with photon energy, consistent with previously reported findings [32]. Additionally,  $\alpha$  also varies with gamma radiation doses. Table-1 presents the absorption coefficient values at 590 nm for  $\text{Se}_{80}\text{In}_5\text{Te}_6\text{Sb}_9$  thin films subjected to different radiation doses. The evaluated absorption coefficient ( $\alpha$ ) values are on the order of  $10^4 \text{ cm}^{-1}$ , aligning well with previously reported results [33-34].

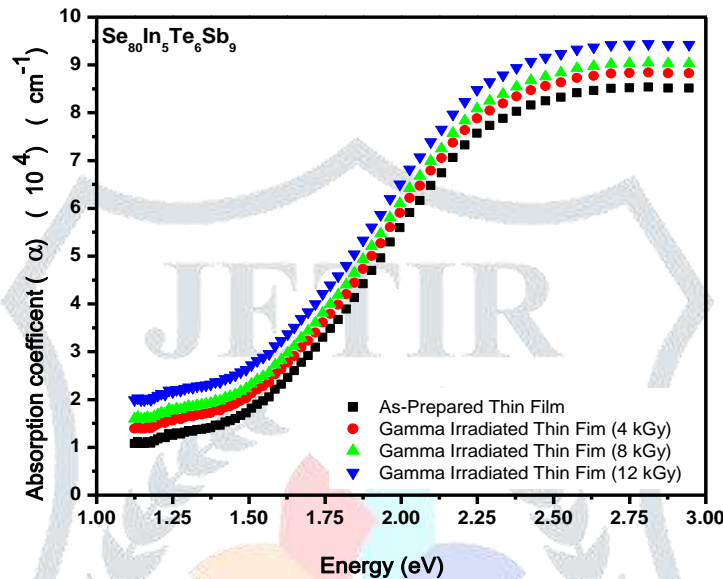


Fig. 4: The plot of absorption coefficient ( $\alpha$ ) versus photon energy ( $h\nu$ ) for as-prepared and  $\gamma$ -irradiated  $\text{Se}_{80}\text{In}_5\text{Te}_6\text{Sb}_9$  thin films.

As we know that, for most chalcogenide glasses the absorption coefficient, energy of incident radiation and band gap is described by the following law [35-36]:

$$(\alpha h\nu)^q = A (h\nu - E_g) \tag{2}$$

Where  $E_g$  is optical band gap,  $q$  is the parameter which decides the band gap nature and  $A$  is a transition probability dependent factor.

We have found the best fit graph for  $\text{Se}_{80}\text{In}_5\text{Te}_6\text{Sb}_9$  thin films for  $q = 1/2$  which indicate that the optical transition is non-direct in nature. The plot of  $(\alpha h\nu)^{1/2}$  versus photon energy ( $h\nu$ ) for as-deposited and  $\gamma$ -irradiated  $\text{Se}_{80}\text{In}_5\text{Te}_6\text{Sb}_9$  thin films is shown in Fig. 5.

**Table 1: Optical parameters in  $\text{Se}_{80}\text{In}_5\text{Te}_6\text{Sb}_9$  chalcogenide thin films**

| $\gamma$ -irradiated doses (kGy) | Optical parameters   |            |  |
|----------------------------------|--|------------|--|
|                                  | $\alpha$ at $\lambda= 590 \text{ nm}$ ( $10^4 \text{ cm}^{-1}$ ) | $E_g$ (eV) | $k$ at $\lambda= 590 \text{ nm}$ ( $10^{-2}$ ) |
| As-prepared                      | 6.71   | 0.95       | 39.08  |
| 4                                | 6.94   | 1.02       | 43.03  |
| 8                                | 7.02   | 1.08       | 47.28  |
| 12                               | 7.33   | 1.12       | 50.29  |

By extrapolating the linear portion of the graph, it intersects the energy axis and this intersection directly provides the value of the optical band gap. The estimated optical band gap values for  $Se_{80}In_5Te_6Sb_9$  thin films are listed in Table-1.

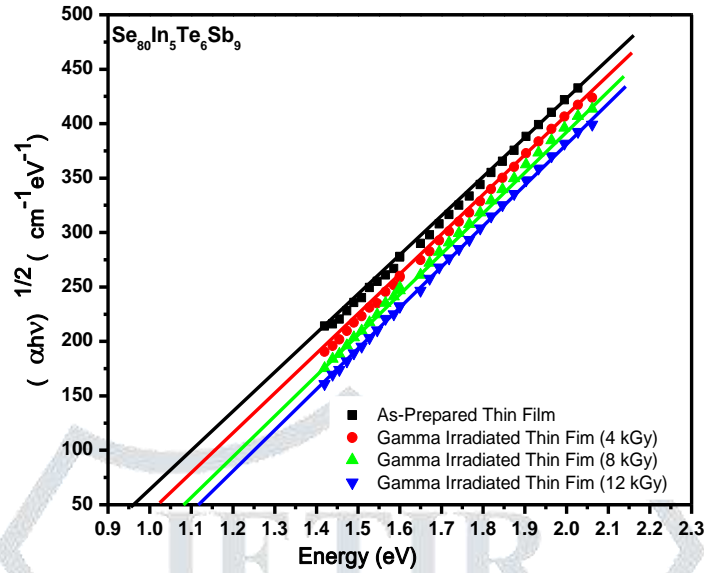


Fig. 5: The plot of  $(\alpha hv)^{1/2}$  versus photon energy  $(hv)$  for as-prepared and Gamma irradiated  $Se_{80}In_5Te_6Sb_9$  thin films.

It is evident from the table that the optical band gap ( $E_g$ ) increases with the dose of incident gamma radiation. Similar observations have been reported by several researchers [37-38].

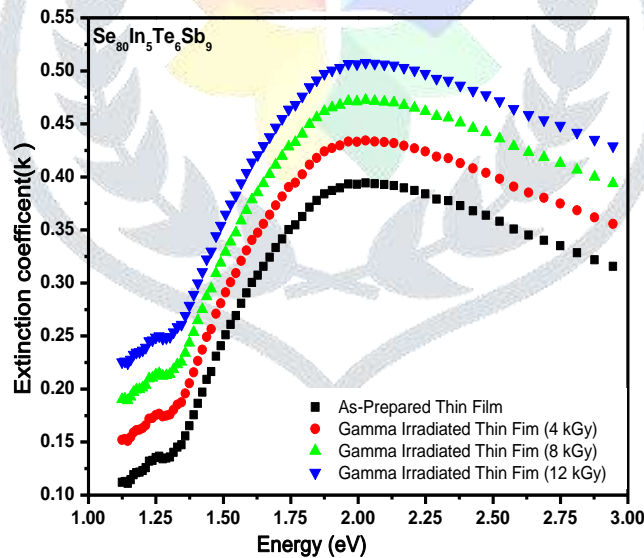


Fig. 6: The plot of extinction coefficient  $(k)$  versus photon energy  $(hv)$  for as-prepared and Gamma irradiated  $Se_{80}In_5Te_6Sb_9$  thin films.

The increase in the optical band gap of  $Se_{80}In_5Te_6Sb_9$  chalcogenide thin films with gamma radiation dose may be attributed to the deterioration of the crystalline structure, accumulation of crystal defects, increased disorder, and enhanced lattice strain.

For various device applications, the extinction coefficient  $(k)$  provides valuable insights into the properties of glassy alloys. The extinction coefficient  $(k)$  is defined as [39]:

$$k = (\alpha\lambda) / (4\pi) \tag{3}$$

The extinction coefficient was determined using the aforementioned equation for both as-prepared and  $\gamma$ -irradiated  $\text{Se}_{80}\text{In}_5\text{Te}_6\text{Sb}_9$  thin films.

Figure 6 illustrates the spectral dependence of the extinction coefficient ( $k$ ) for  $\text{Se}_{80}\text{In}_5\text{Te}_6\text{Sb}_9$  chalcogenide thin films. The plots reveal that the values of extinction coefficient increase with the incident photon energy. Extinction coefficient is found to vary with different radiation doses which designating about the variation in defect states with radiation dose [40]. The calculated values of extinction coefficient at 590 nm wavelength are encapsulated in Table 1. The variation may be due to presence of unsaturated bonds which lead to localized states and affects the extinction coefficient.

#### 4. Conclusions

This study investigates the phase transformation studies in  $\text{Se}_{80}\text{In}_5\text{Te}_6\text{Sb}_9$  chalcogenide thin films by  $\gamma$ -irradiation. DSC measurements were used to confirm the amorphous and glassy nature of the synthesized alloy. HRXRD and FESEM analyses corroborate the amorphous structure of the as-prepared films and reveal phase transformations induced by gamma irradiation. Optical absorption measurements reveal that the absorption process in  $\text{Se}_{80}\text{In}_5\text{Te}_6\text{Sb}_9$  thin films is governed by indirect electronic transitions. It was observed that the optical band gap decreases with increasing  $\gamma$ -irradiation dose, indicating the formation of localized states within the band structure. Both the absorption coefficient and extinction coefficient ( $k$ ) exhibit an increasing trend with rising photon energy, suggesting enhanced photon-material interactions at higher energies. The observed decrease in the optical band gap with increasing  $\gamma$ -irradiation doses can be attributed to the introduction of defect states within the band structure, leading to a shift in the Fermi level. This shift is influenced by the redistribution of electrons over these localized states. Outcome of these studies suggest that it is possible to modulate the band gap of the material, offering potential for tailoring its properties for various optoelectronic devices.

#### Acknowledgements:

The authors express her sincere gratitude to Prof. M. Zulfequar, Department of Physics, Jamia Millia Islamia, New Delhi, India, for providing access to experimental facilities in his research laboratory and Centre for Nanoscience and Nanotechnology, as well as for his insightful discussions and valuable suggestions throughout the writing of this research

#### References:

- [1] B. J. Eggleton, *Opt. Express* 18 (2010) 26632.
- [2] B. J. Eggleton, B. Luther-Davies, K. Richardson, *Nat. Photonics* 5 (2011) 141.
- [3] C. Conseil, Q. Coulombier, J. Trolesa, L. Brilland, G. Renversez, D. Mechinh, B. Bureau, J. L. Adam, J. Lucas, *J. Non-Cryst. Solids* 357(11–13) (2011) 2480.
- [4] N. Mehta, *J. Scien. Indus. Research*. 65 (2006) 777.
- [5] V. A. Danko, I. Z. Indutnyi, M.V. Lykanyuk, V.I. Minko, Shepeliavyi, *Science and Innovation*. 10(5) (2014) 22.
- [6] Y. Zhai, R. Qi, C. Yuan, W. Zhang, Y. Huang, *Applied Physics Express*. 9 (2016) 052201(1-3).
- [7] S. M. Kwon, J. K. Won, J-W. Jo, J. Kim, H. J. Kim, H. I. Kwon, J. Kim, S. Ahn, Y. H. Kim, M. J. Lee, H. I. Lee, T. J. Marks, M. G. Kim, and S .K. Park, *Science Advances*. 4(4) (2018) eaap 9104.
- [8] H. Qiu, C. Jiang, G. Li, D. Hao, X. Yu, Y. Sun, *J. Nanoelectronics and Optoelectronics*. 16 (9) (2021)1501–1509.

- [9] T. K. Todorov, J. Tang, S. Bag, O. Gunawan, T. Gokmen, Y. Zhu, and D. B. Mitzi, *Advanced Energy Materials*. 3(1) (2013) 34–38.
- [10] M. Suhail, H. Abbas, M. B. Khan, Z. H. Khan, *J. of Nanoparticle Research*. 24(7) (2022) 142.
- [11] C. Shen, T. Li, Y. Zhang, R. Xie, T. Long, N. M. Fortunato, F. Liang, M. Dai, J. Shen, C. M. Wolverton, H. Zhang, *J. American Chemical Society*. 145(40) (2023) 21925–21936.
- [12] S. Y. Lee, Y. H. Kim, S. M. Cho, G. H. Kim, T. Y. Kim, H. Ryu, H. N. Kim, H. B. Kang, C. Y. Hwang, C. S. Hwang, *Scientific Reports*. 7(1) (2017) 41152.
- [13] L. Li, H. Lin, S. Qiao, Y. Zou, S. Danto, K. Richardson, J. D. Musgraves, N. Lu, and J. Hu, *Nature Photonics*. 8(8) (2014) 643-649.
- [14] P. Phogat, Shreya, R. Jha, S. Singh, *Engg. and Technology Journal*. 9(7) (2024) 4580-4606.
- [15] D. Sahoo, R. Naik, *J. of Non-Crystalline Solids*, 597 (2022) 121934.
- [16] Archana Srivastava, S. N. Tiwari, J. K. Lal, Shamshad A. Khan, *Glass Physics and Chemistry* 45 (2019) 111-118.
- [17] S. Cui, R. Chahal, C. Boussard Pleedel, V. Nazabal, J. L. Doualan, J. Louis, J. Troles, J. Lucas, B. Bureau, *Molecules*. 18(5) (2013) 5373-5388.
- [18] R. Chbeir et al, *Journal of the American Ceramic Society*. 106(6) (2023) 3277-3302.
- [19] M. El-Hagary, M. Emam-Ismail, E. R. Shaaban, A. El-Taher, *Radiation Physics and Chemistry*. 81(10) (2012) 1572-1577.
- [20] S. Ahmad, S. Islam, K. Asokan, M. Zulfequar, *J. Phy. and Chem. of Solids* 117 (2018) 122.
- [21] M. Shpotyuk, A. Kovalskiy, O. Shpotyuk, *J. Non-Cryst. Solids* 498 (2018) 315.
- [22] K. A. Aly, A. Dahshan, Y. Saddeek, *J. of Mat. Science: Mat. in Electronics*. 33(16) (2022) 12663.
- [23] A. M. Abdul-Kader, Y. A. El-Gendy, *Nuclear Instruments and Methods in Physics Research Section B: Beam Interactions with Materials and Atoms*. 305 (2013) 22.
- [24] M. A. Al-Ewaisi, M. M. A. Imran, O. A. Lafi, M. W. Kloub, *Physica B* 405(12) (2010) 2643.
- [25] Saeid M. Elkatlawy, Ahmed H. El-Dosokey, Hossam M. Gomaa, *Boletín de la Sociedad Española de Cerámica y Vidrio*. 61(3) (2022) 203.
- [26] S. Joshi, N. K. Udayashankar, *J. Materials Science: Materials in Electronics*, 35(12) (2024) 828.
- [27] Anjali, B. S. Patial, P. Sharma, N. Thakur, *Journal of Materials Science: Materials in Electronics*, 34(26) (2023) 1833.
- [28] S. A. Khan, I. H. Khan, M. S. Akhtar, I. Ekmekci, T.G. Kim, M. Hashem, N. M. Alfrisany, H. Fouad, A. Srivastava, *Science of Advanced Materials*. 15(3) (2023) 434–440.
- [29] N. K. Abdalameer, S. N. Mazhir, K. A. Aadim. *Energy Reports*. 6 (2020) 447-458.
- [30] S. A. Khan, R. M. Sahani, R. P. Tripathi, M. S. Akhtar, A. Srivastava. *Radiation Physics and Chemistry*. 188 (2021) 109659.
- [31] R. P. Tripathi, M. A. Alvi, S. A. Khan, *J. of Thermal Analysis and Calorimetry*, 146(5) (2021) 2261-2272.
- [32] R. P. Tripathi, M. S. Akhtar, M. A. Alvi, S. A. Khan, *Journal of Materials Science: Materials in Electronics*. 27 (8) (2016) 8227-8233.
- [33] I. Sharma, P. Sharma, A. S. Hassaniien, *J. of Non-Crystalline Solids*. 590 (2022) 121673.
- [34] D. Sahoo and R. Naik, *Journal of Non-Crystalline Solids*, 597 (2022) 121934.

- [35] S. Agarwal, P. Lohia, D. K. Dwivedi, Journal of Non-Crystalline Solids. 606 (2023) 122199.
- [36] Y. B. Singh et al, Materials Chemistry and Physics. 274 (2021) 125153.
- [37] H. E. Atyia, S. S. Fouad, S. Kumar Pal, A. Srivastava, N. Mehta, Optics & Laser Technology. 150 (2022) 107985.
- [38] A. S. Hassanien, I. Sharma, P. Sharma, Materials Chemistry and Physics. 293 (2023) 126887.
- [39] A. Srivastava, Z. H. Khan, S. A. Khan, J. of Physics D: Applied Physics. 57( 9) (2024) 95303.
- [40] D. Biswas, R. Mondal, D. Mandal, S. Mondal, J. of Non-Crystalline Solids. 614 (2023) 122401.

